Acta Cryst E CRYSTALLOGRAPHIC COMMUNICATIONS
ISSN 2056-9890

Crystal structures and comparisons of huntite aluminum borates $RE\mathrm{Al_3(BO_3)_4}$ (RE = Tb, Dy and Ho)

Saehwa Chong,[a]* Brian J. Riley,[a] Zayne J. Nelson[a] and Samuel N. Perry[b]

[a]Pacific Northwest National Laboratory, Richland, WA 99354, USA, and [b]Department of Civil and Environmental Engineering and Earth Sciences, University of Notre Dame, Notre Dame, IN 46556, USA. *Correspondence e-mail: saehwa.chong@pnnl.gov

Received 28 January 2020
Accepted 7 February 2020

Edited by P. Roussel, ENSCL, France

Keywords: huntite borate; lanthanide aluminum borate; single-crystal XRD.

CCDC references: 1983041; 1983040; 1983039

Supporting information: this article has supporting information at journals.iucr.org/e

Three huntite-type aluminoborates of stoichiometry $RE\mathrm{Al_3(BO_3)_4}$ (RE = Tb, Dy and Ho), namely, terbium/dysprosium/holmium trialuminium tetrakis(borate), were synthesized by slow cooling within a $\mathrm{K_2Mo_3O_{10}}$ flux with spontaneous crystallization. The crystal structures were determined using single-crystal X-ray diffraction (SC-XRD) data. The synthesized borates are isostructural to the huntite [$\mathrm{CaMg_3(CO_3)_4}$] structure and crystallized within the trigonal $R32$ space group. The structural parameters were compared to literature data of other huntite $RE\mathrm{Al_3(BO_3)_4}$ crystals within the $R32$ space group. All three borates fit well into the trends calculated from the literature data. The unit-cell parameters and volumes increase linearly with larger RE cations whereas the densities decrease. All of the crystals studied were refined as inversion twins.

1. Chemical context

Rare-earth aluminum borates (REAB) with the general chemical formula $RE\mathrm{Al_3(BO_3)_4}$ (RE = La, Pr, Nd, Sm, Eu, Gd, Tb, Dy, Ho, Er, Tm, Yb, Lu, Y) have been studied extensively for applications in lasers, nonlinear optics, sensors, and phosphors because of their optical and magnetoelectric properties as well as the capacity to be doped with other rare-earth metals (Koporulina *et al.*, 2000; Leonyuk & Leonyuk, 1995; Leonyuk *et al.*, 1998; Mills, 1962; Belokoneva & Timchenko, 1983; Belokoneva, 1994). The REAB crystals are promising materials for self-frequency-doubling lasers as their nonlinear optical properties can be changed by doping with different rare-earth elements including Nd, Dy, Er, Yb, Tm, or Y (Leonyuk *et al.*, 1998, 2007; Földvári *et al.*, 2003; Chen *et al.*, 2012). The REAB compounds with RE = Tb, Ho, Er, or Tm exhibit the magnetoelectric properties useful for sensor applications (Liang *et al.*, 2011, 2012), and REAB with the RE = Pr, Sm, Eu, Gd, Tb, or Ho can be used as phosphors (Li & Wang, 2007; He *et al.*, 2015).

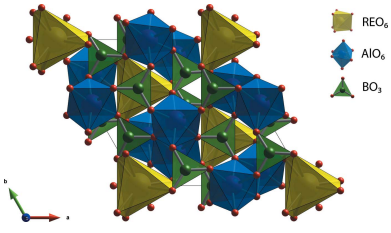

The REAB compounds are generally synthesized by a flux-assisted growth method with or without seeds at 800–1150°C (Leonyuk & Leonyuk, 1995; Koporulina *et al.*, 2000; Wang, 2012; Leonyuk, 2017). The $\mathrm{K_2Mo_3O_{10}}$ (Tu *et al.*, 1994; Wang *et al.*, 1995; Leonyuk & Leonyuk, 1995; Teshima *et al.*, 2006) compound is the most commonly used flux for the crystallization of REAB, although other fluxes such as $\mathrm{Bi_2O_3}$–$\mathrm{B_2O_3}$ (Chani *et al.*, 1994) and BaO–$\mathrm{B_2O_3}$ (Jung *et al.*, 1995) have been used. Two major drawbacks of using the $\mathrm{K_2Mo_3O_{10}}$ flux are the potential incorporation of Mo into the REAB structure and co-crystallization of other phases (Wang, 2012;

Leonyuk, 2017; Kuz'micheva *et al.*, 2019). In the current study, $K_2Mo_3O_{10}$ flux was used to synthesize $RE Al_3(BO_3)_4$ (*RE* = Tb, Dy, Ho) crystals, and the structural parameters of the synthesized REAB crystals were compared to literature data.

2. Structural commentary

The crystal structures of the synthesized REAB crystals are isostructural to the huntite structure (Mills, 1962) with the *R*32 space group (Fig. 1). The huntite aluminoborates generally crystallize within the *R*32 space group; however, REAB compounds with *RE* = Pr, Nd, Sm, Eu, Tb, Ho, or Gd showed the transition in space group from *R*32 to lower symmetry monoclinic *C*2/*c* and *C*2 space groups in the disordered structures caused by variations in the growth temperature, cooling rate, and composition (Belokoneva & Timchenko, 1983; Belokoneva *et al.*, 1988, 1994; Leonyuk & Leonyuk, 1995; Plachinda & Belokoneva, 2008; Leonyuk, 2017). The structures of the REAB crystals are composed of rare-earth cations with a distorted trigonal–prismatic coordination (REO_6), aluminum cations with a distorted octahedral coordination (AlO_6), and boron cations with a trigonal–planar coordination (BO_3) as shown in Fig. 2. The AlO_6 octahedra form helical chains along the *c*-axis direction by sharing edges, and these chains are connected by BO_3 units (see Fig. 3).

The structural parameters of the synthesized REAB compounds were added to literature data for comparison (see Fig. 4), and they were in good agreement when plotted *versus* the average ionic crystal radius of the six-coordinated RE element according to Shannon (1976). The trendlines show that the unit-cell parameters and volumes increase linearly whereas the densities decrease with the larger rare-earth cations in the structures. The data included in Fig. 4 include literature data for $RE Al_3(BO_3)_4$ where *RE* = Pr, Nd, Sm, Eu, Gd, Tb, Dy, Ho, Er, Tm, Yb, or Lu, as well as mixtures of Y/Er and Y/Nd (Belokoneva *et al.*, 1981; Hong & Dwight, 1974; Xu *et al.*, 2002; Jia *et al.*, 2006; Kuroda *et al.*, 1981; Leonyuk & Leonyuk, 1995; Malakhovskii *et al.*, 2014; Mészáros *et al.*, 2000; Mills, 1962; Plachinda & Belokoneva, 2008; Prokhorov *et al.*, 2013, 2014; Sváb *et al.*, 2012; Wang *et al.*, 1991).

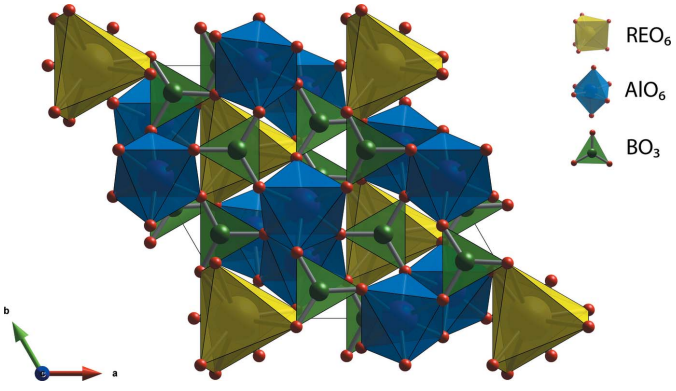

Figure 1
Crystal structure of $RE Al_3(BO_3)_4$.

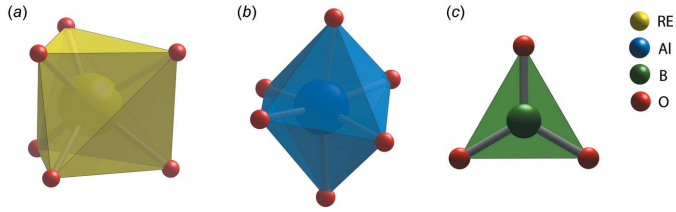

Figure 2
Coordination of oxygen atoms around (*a*) rare-earth, (*b*) aluminum, and (*c*) boron atoms shown as polyhedra.

3. Synthesis and crystallization

The REAB single crystals were synthesized using Tb_2O_3 (Alfa Aesar, 99.9%), Dy_2O_3 (Alfa Aesar, 99.9%), Ho_2O_3 (Alfa Aesar, 99.9%), $Al(OH)_3$ (Almatis, 99.5%), B_2O_3 (Alfa Aesar, 99.98%), and $K_2Mo_3O_{10}$ flux. All the rare-earth oxides, $Al(OH)_3$, and B_2O_3 were used as received; the B_2O_3 was stored and handled in a nitrogen glovebox to prevent hydration (M-Braun, Inc., < 0.1 ppm of O_2 and H_2O). The $K_2Mo_3O_{10}$ flux was synthesized using K_2CO_3 (Alfa Aesar, 99%) and MoO_3 (Alfa Aesar, 99.5%). For the flux, appropriate amounts of K_2CO_3 and MoO_3 were mixed in a mortar and pestle and placed into a Pt/10%Rh crucible. The crucible was heated to 520°C at 5°C min^{-1}, maintained at that temperature for 8 h, and then cooled down to room temperature at 5°C min^{-1}. For the synthesis of the REAB crystals, the rare-earth oxide was mixed with $Al(OH)_3$ and B_2O_3 in a 1:6:5 molar ratio, and then $K_2Mo_3O_{10}$ was added at 40 mass% of the total precursor mass. The mixed powder of each rare-earth element was put into a Pt/10%Rh crucible, tightly covered with a Pt/10%Rh lid, and placed in a Thermolyne box furnace. The furnace was heated to 900°C at 5°C

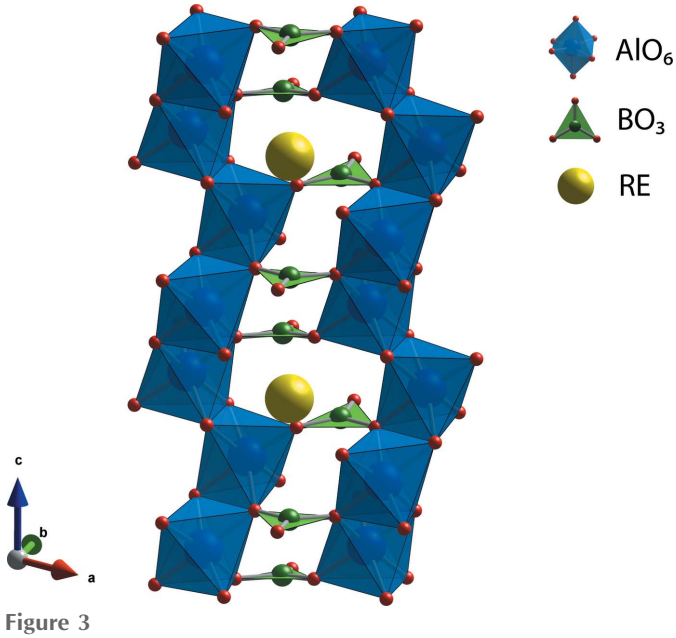

Figure 3
Structure showing the helical chains composed of edge sharing AlO_6 units along the *c* axis connected by BO_3 in $RE Al_3(BO_3)_4$.

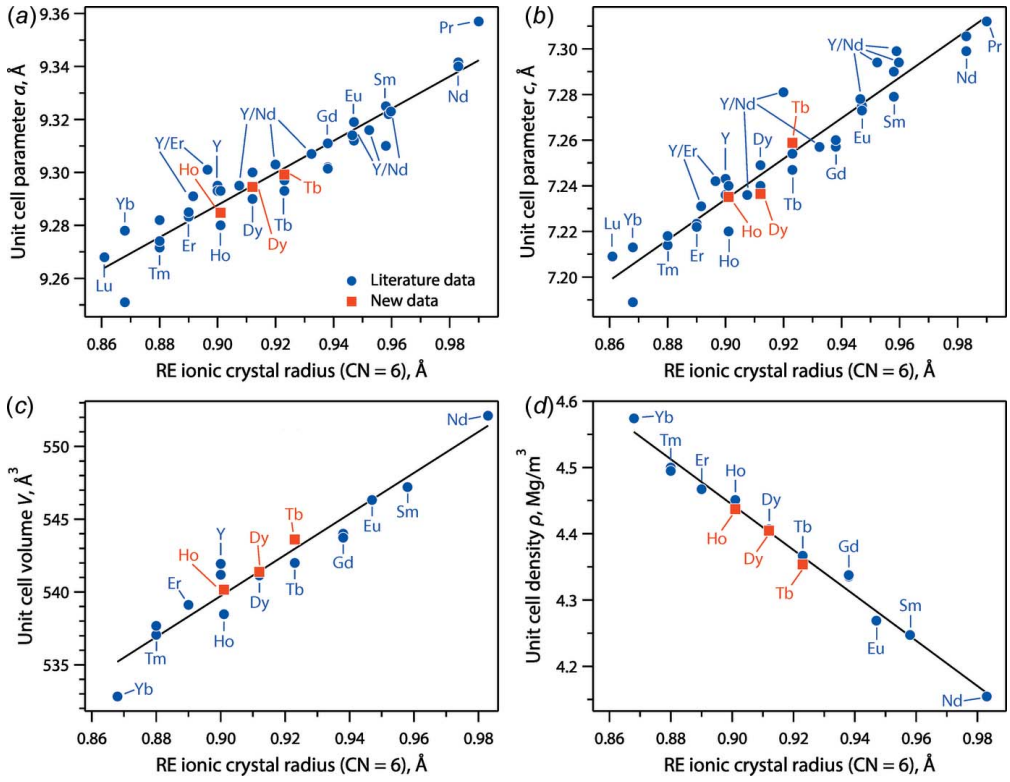

Figure 4
Summary of (*a*) unit-cell parameter *a*, (*b*) unit-cell parameter *c*, (*c*) unit-cell volume (*V*), and (*d*) density (ρ) as a function of the average ionic crystal radii of the *RE* in the crystal structures (coordination number = 6) from Shannon (1976).

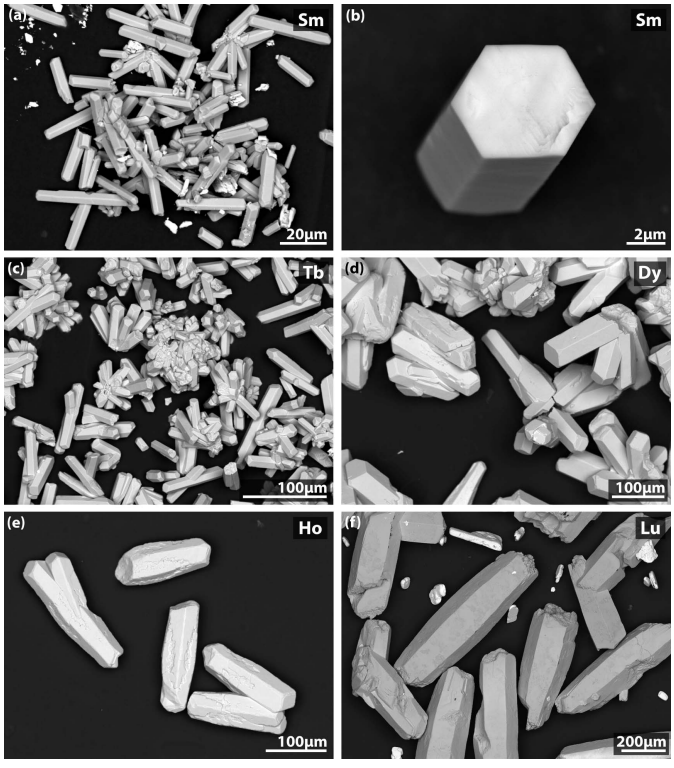

Figure 5
Back-scattered electron SEM micrographs of $RE\mathrm{Al_3(BO_3)_4}$ crystals including (*a*) and(*b*) $\mathrm{SmAl_3(BO_3)_4}$, (*c*) $\mathrm{TbAl_3(BO_3)_4}$, (*d*) $\mathrm{DyAl_3(BO_3)_4}$, (*e*) $\mathrm{HoAl_3(BO_3)_4}$, and (*f*) $\mathrm{LuAl_3(BO_3)_4}$. Note that some $\mathrm{KLu(MoO_4)_2}$ crystals are seen in (*a*) and (*d*) as the smaller and brighter crystallites.

min^{-1}, maintained at that temperature for 4 h, cooled to 400°C at 5°C h^{-1}, and then shut off to cool naturally. The synthesized products were washed with deionized water in a sonic bath, and the crystals were recovered with vacuum filtration using a Büchner funnel. The REAB crystals along with $\mathrm{KRE(MoO_4)_2}$ were synthesized by this process as expected from previous studies (Leonyuk *et al.*, 1998; Teshima *et al.*, 2006; Leonyuk, 2017; Kuz'micheva *et al.*, 2019).

The REAB crystals generally have hexagonal prismatic shapes, and they were often agglomerated (Fig. 5), as observed with scanning electron microscopy (JSM-7001F field emission gun SEM; JEOL USA, Inc.). Crystals of $\mathrm{SmAl_3(BO_3)_4}$ and $\mathrm{LuAl_3(BO_3)_4}$ were also grown using the same procedure as described above and these are shown in Fig. 5 for comparison; however, the crystal structures are not reported due to the poor diffraction of $\mathrm{SmAl_3(BO_3)_4}$ and unresolvable displacement parameters during structural refinement for $\mathrm{LuAl_3(BO_3)_4}$. Finally, for the crystal growth conditions used here, the average crystallite sizes for the different $\mathrm{REAl_3(BO_3)_4}$ crystals herein (*RE* = Sm, Tb, Dy, Ho, Lu) are shown in Fig. 6 with standard deviations based on measurements of ≥ 7 crystals from each sample.

4. Refinement

Crystal data, data collection and structure refinement details are summarized in Table 1. Suitable crystals were selected for SC-XRD and were placed on cryoloops in oil (Parabar 10312,

Table 1
Experimental details.

	Tb-borate	Dy-borate	Ho-borate
Crystal data			
Chemical formula	$TbAl_3(BO_3)_4$	$DyAl_3(BO_3)_4$	$HoAl_3(BO_3)_4$
M_r	475.1	478.7	481.1
Crystal system, space group	Trigonal, *R*32	Trigonal, *R*32	Trigonal, *R*32
Temperature (K)	100	100	100
a, *c* (Å)	9.2992 (8), 7.2588 (7)	9.2938 (5), 7.2348 (4)	9.2832 (3), 7.2345 (3)
V (Å^3)	543.61 (8)	541.18 (5)	539.93 (3)
Z	3	3	3
Radiation type	Mo *Kα*	Mo *Kα*	Mo *Kα*
μ (mm^{-1})	10.21	10.81	11.45
Crystal size (mm)	0.03 × 0.03 × 0.02	0.05 × 0.05 × 0.03	0.05 × 0.05 × 0.03
Data collection			
Diffractometer	Bruker D8 QUEST CMOS area detector	Bruker D8 QUEST CMOS area detector	Bruker D8 QUEST CMOS area detector
Absorption correction	Multi-scan (*SADABS*; Krause *et al.*, 2015)	Multi-scan (*SADABS*; Krause *et al.*, 2015)	Multi-scan (*SADABS*; Krause *et al.*, 2015)
T_{min}, T_{max}	0.530, 0.747	0.588, 0.723	0.570, 0.709
No. of measured, independent and observed [$I > 2\sigma(I)$] reflections	6957, 270, 270	7295, 420, 420	5662, 381, 381
R_{int}	0.113	0.044	0.047
Refinement			
$R[F > 3\sigma(F)]$, $wR(F)$, S	0.020, 0.021, 1.08	0.010, 0.010, 1.14	0.012, 0.015, 1.08
No. of reflections	270	420	381
No. of parameters	32	35	35
$\Delta\rho_{max}$, $\Delta\rho_{min}$ (e Å^{-3})	0.59, −0.88	0.29, −0.39	0.54, −0.65
Absolute structure	Refined as an inversion twin with a twin ratio of 0.51 (2):0.49 (2)	Refined as an inversion twin with a twin ratio of 0.509 (8):0.491 (8)	Refined as an inversion twin with a twin ratio of 0.558 (12):0.442 (12)
Absolute structure parameter	0.49 (2)	0.491 (8)	0.442 (12)

Computer programs: *APEX3* and *SAINT* (Bruker, 2012), *JANA2006* (Petříček *et al.*, 2014), *SUPERFLIP* (Palatinus & Chapuis, 2007), *VESTA* (Momma & Izumi, 2011) and *publCIF* (Westrip, 2010).

Hampton Research). Data were collected with a scan width of 0.5° in φ and ω with a 10 sec dwell time per frame at 100 K. All the REAB crystals had chiral structures and were refined with inversion twinning. The final refinements for $TbAl_3(BO_3)_4$, $DyAl_3(BO_3)_4$, and $HoAl_3(BO_3)_4$ converged at R_1 = 1.97% with goodness-of-fit of 1.08, R_1 = 0.80% with goodness-of-fit of 1.14, and R_1 = 1.15% with goodness-of-fit of 1.08, respectively.

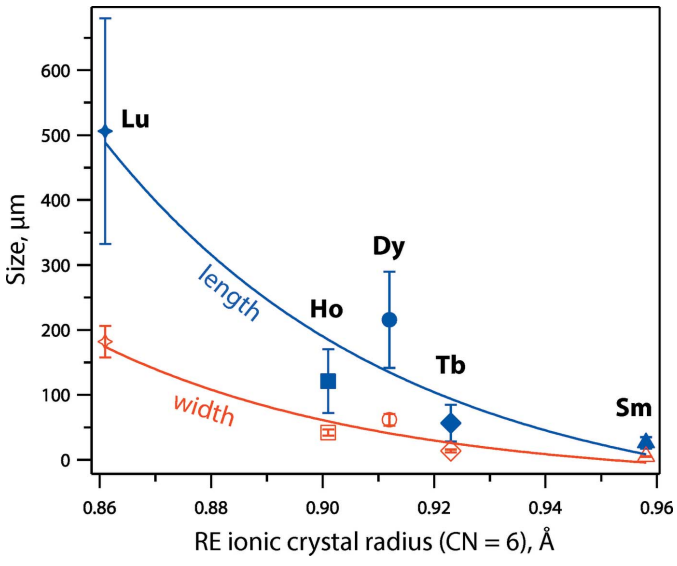

Figure 6
Summary of crystal size in terms of average length and width as a function of the average ionic crystal radii of the *RE* in the crystal structures (coordination number = 6) from Shannon (1976).

Acknowledgements

The Pacific Northwest National Laboratory is operated by Battelle under Contract Number DE-AC05–76RL01830.

Funding information

The authors acknowledge financial support from the US Department of Energy Office of Nuclear Energy (DOE-NE).

References

Belokoneva, E. L. (1994). *Russ. Chem. Rev.* **63**, 533–549.
Belokoneva, E. L., Azizov, A. V., Leonyuk, N. I., Simonov, M. A. & Belov, N. V. (1981). *J. Struct. Chem.* **22**, 476–478.
Belokoneva, E. L., Leonyuk, N. I., Pashkova, A. V. & Timchenko, T. I. (1988). *Kristallografiya*, **33**, 1287–1288.
Belokoneva, E. L. & Timchenko, T. I. (1983). *Kristallografiya*, **28**, 1118–1123.
Bruker (2012). *SAINT*. Bruker AXS Inc., Madison, Wisconsin, USA.
Chani, V. I., Shimamura, K., Inoue, K., Sasaki, T. & Fukuda, T. (1994). *Jpn. J. Appl. Phys.* **33**, 247–250.
Chen, Y., Lin, Y., Gong, X., Huang, J., Luo, Z. & Huang, Y. (2012). *Opt. Lett.* **37**, 1565–1567.
Földvári, I., Beregi, E., Baraldi, A., Capelletti, R., Ryba-Romanowski, W., Dominiak-Dzik, G., Munoz, A. & Sosa, R. (2003). *J. Lumin.* **102–103**, 395–401.

He, J., Zhang, S., Zhou, J., Zhong, J., Liang, H., Sun, S., Huang, Y. & Tao, Y. (2015). *Opt. Mater.* **39**, 81–85.
Hong, H.-P. & Dwight, K. (1974). *Mater. Res. Bull.* **9**, 1661–1665.
Jia, G., Tu, C., Li, J., You, Z., Zhu, Z. & Wu, B. (2006). *Inorg. Chem.* **45**, 9326–9331.
Jung, S. T., Choi, D. Y., Kang, J. K. & Chung, S. J. (1995). *J. Cryst. Growth*, **148**, 207–210.
Koporulina, E. V., Leonyuk, N. I., Mokhov, A. V., Pilipenko, O. V., Bocelli, G. & Righi, L. (2000). *J. Cryst. Growth*, **211**, 491–496.
Krause, L., Herbst-Irmer, R., Sheldrick, G. M. & Stalke, D. (2015). *J. Appl. Cryst.* **48**, 3–10.
Kuroda, R., Mason, S. F. & Rosini, C. (1981). *J. Chem. Soc. Faraday Trans. 2*, **77**, 2125–2140.
Kuz'micheva, G. M., Kaurova, I. A., Rybakov, V. B. & Podbel'skiy, V. V. (2019). *Crystals*, **9**, 100.
Leonyuk, N. I. (2017). *J. Cryst. Growth*, **476**, 69–77.
Leonyuk, N. I., Koporulina, E. V., Barilo, S. N., Kurnevich, L. A. & Bychkov, G. L. (1998). *J. Cryst. Growth*, **191**, 135–142.
Leonyuk, N. I. & Leonyuk, L. I. (1995). *Prog. Cryst. Growth Charact. Mater.* **31**, 179–278.
Leonyuk, N. I., Maltsev, V. V., Volkova, E. A., Pilipenko, O. V., Koporulina, E. V., Kisel, V. E., Tolstik, N. A., Kurilchik, S. V. & Kuleshov, N. V. (2007). *Opt. Mater.* **30**, 161–163.
Li, X. & Wang, Y. (2007). *J. Lumin.* **122–123**, 1000–1002.
Liang, K. C., Chaudhury, R. P., Lorenz, B., Sun, Y. Y., Bezmaternykh, L. N., Gudim, I. A., Temerov, V. L. & Chu, C. W. (2012). *J. Phys. Conf. Ser.* **400**, 032046.
Liang, K.-C., Chaudhury, R. P., Lorenz, B., Sun, Y. Y., Bezmaternykh, L. N., Temerov, V. L. & Chu, C. W. (2011). *Phys. Rev. B*, **83**, 180417.
Malakhovskii, A. V., Kutsak, T. V., Sukhachev, A. L., Aleksandrovsky, A. S., Krylov, A. S., Gudim, I. A. & Molokeev, M. S. (2014). *Chem. Phys.* **428**, 137–143.
Mészáros, G., Sváb, E., Beregi, E., Watterich, A. & Tóth, M. (2000). *Physica B*, **276–278**, 310–311.
Mills, A. (1962). *Inorg. Chem.* **1**, 960–961.
Momma, K. & Izumi, F. (2011). *J. Appl. Cryst.* **44**, 1272–1276.
Palatinus, L. & Chapuis, G. (2007). *J. Appl. Cryst.* **40**, 786–790.
Petříček, V., Dusek, M. & Palatinus, L. (2014). *Z. Kristallogr.* **229**, 345–352.
Plachinda, P. A. & Belokoneva, E. L. (2008). *Cryst. Res. Technol.* **43**, 157–165.
Prokhorov, A. D., Prokhorov, A. A., Chernush, L. F., Minyakaev, R., Dyakonov, V. P. & Szymczak, H. (2014). *Phys. Status Solidi B*, **251**, 201–205.
Prokhorov, A. D., Zubov, E. E., Prokhorov, A. A., Chernush, L. F., Minyakaev, R., Dyakonov, V. P. & Szymczak, H. (2013). *Phys. Status Solidi B*, **250**, 1331–1338.
Shannon, R. D. (1976). *Acta Cryst.* A**32**, 751–767.
Sváb, E., Beregi, E., Fábián, M. & Mészáros, G. (2012). *Opt. Mater.* **34**, 1473–1476.
Teshima, K., Kikuchi, Y., Suzuki, T. & Oishi, S. (2006). *Cryst. Growth Des.* **6**, 1766–1768.
Tu, C., Luo, Z., Chen, G. & Wang, G. (1994). *Cryst. Res. Technol.* **29**, K47–K50.
Wang, G., Gallagher, H. G., Han, T. P. J. & Henderson, B. (1995). *J. Cryst. Growth*, **153**, 169–174.
Wang, G., Meiyun, H. & Luo, Z. (1991). *Mater. Res. Bull.* **26**, 1085–1089.
Wang, G.-F. (2012). *Structure–Property Relationships in Non-Linear Optical Crystals I*, pp. 105-119. Berlin, Heidelberg: Springer.
Westrip, S. P. (2010). *J. Appl. Cryst.* **43**, 920–925.
Xu, Y. Y., Chen, Y. J., Luo, Z. D., Chen, J. T. & Huang, Y. D. (2002). *Chin. J. Struct. Chem.* **21**, 402–404.

supporting information

Acta Cryst. (2020). E**76**, 339-343 [https://doi.org/10.1107/S2056989020001802]

Crystal structures and comparisons of huntite aluminum borates $RE\mathrm{Al_3(BO_3)_4}$ (RE = Tb, Dy and Ho)

Saehwa Chong, Brian J. Riley, Zayne J. Nelson and Samuel N. Perry

Computing details

For all structures, data collection: *APEX3* (Bruker, 2012); cell refinement: JANA2006 (Petříček *et al.*, 2014); data reduction: *SAINT* (Bruker, 2012); program(s) used to solve structure: SUPERFLIP (Palatinus & Chapuis, 2007); program(s) used to refine structure: JANA2006 (Petříček *et al.*, 2014); molecular graphics: *VESTA* (Momma & Izumi, 2011); software used to prepare material for publication: *publCIF* (Westrip, 2010).

Terbium trialuminium tetrakis(borate) (Tb-borate)

Crystal data

$TbAl_3(BO_3)_4$
M_r = 475.1
Trigonal, $R32$
Hall symbol: R 3 2"
a = 9.2992 (8) Å
c = 7.2588 (7) Å
V = 543.61 (8) Å^3
Z = 3
$F(000)$ = 660
D_x = 4.354 Mg m^{-3}
Mo $K\alpha$ radiation, λ = 0.71075 Å
Cell parameters from 6957 reflections
θ = 3.8–33.2°
μ = 10.21 mm^{-1}
T = 100 K
Hexagonal prism, light white
0.03 × 0.03 × 0.02 mm

Data collection

Bruker D8 QUEST CMOS area detector diffractometer
Radiation source: X-ray tube
φ and ω scans
Absorption correction: multi-scan (SADABS; Krause *et al.*, 2015)
T_{min} = 0.530, T_{max} = 0.747
6957 measured reflections
270 independent reflections
270 reflections with $I > 2\sigma(I)$
R_{int} = 0.113
θ_{max} = 33.2°, θ_{min} = 3.8°
h = −13→14
k = −14→13
l = −11→11

Refinement

Refinement on F
$R[F > 3\sigma(F)]$ = 0.020
$wR(F)$ = 0.021
S = 1.08
270 reflections
32 parameters
0 restraints
0 constraints
Primary atom site location: iterative
Weighting scheme based on measured s.u.'s $w = 1/(\sigma^2(F) + 0.0001F^2)$
$(\Delta/\sigma)_{max}$ = 0.041
$\Delta\rho_{max}$ = 0.59 e Å^{-3}
$\Delta\rho_{min}$ = −0.88 e Å^{-3}
Absolute structure: Data was refined with inversion twinning in JANA2006, and the twin ratio was 0.51(2):0.49(2).
Absolute structure parameter: 0.49 (2)

Special details

Refinement. Data was refined with inversion twinning, and the twin ratio was 0.51 (2):0.49 (2).

Fractional atomic coordinates and isotropic or equivalent isotropic displacement parameters (Å²)

	x	*y*	*z*	U_{iso}*/U_{eq}
Tb1	0	0	0	0.01126 (13)
Al1	0.5557 (2)	0	0	0.0052 (6)
B1	0.666667	0.333333	−0.166667	0.0054 (19)
O1	0.7418 (7)	0.0752 (7)	0.166667	0.012 (2)
O2	0.3668 (5)	−0.1151 (5)	−0.1448 (5)	0.0098 (12)
O3	0.8151 (5)	0.4818 (5)	−0.166667	0.0091 (14)
B2	0.8912 (11)	0.2245 (11)	0.166667	0.0066 (12)*

Atomic displacement parameters (Å²)

	U^{11}	U^{22}	U^{33}	U^{12}	U^{13}	U^{23}
Tb1	0.01027 (16)	0.01027 (16)	0.0133 (2)	0.00513 (8)	0	0
Al1	0.0040 (6)	0.0036 (8)	0.0078 (9)	0.0018 (4)	0.0005 (3)	0.0010 (6)
B1	0.004 (2)	0.004 (2)	0.008 (3)	0.0021 (12)	0	0
O1	0.007 (2)	0.007 (2)	0.017 (3)	0.000 (2)	0.0008 (9)	−0.0008 (9)
O2	0.0082 (16)	0.0086 (15)	0.0123 (15)	0.0039 (13)	0.0003 (12)	−0.0013 (12)
O3	0.0075 (15)	0.0075 (15)	0.011 (2)	0.0031 (18)	−0.0010 (8)	0.0010 (8)

Geometric parameters (Å, º)

Tb1—O2^{i}	2.336 (4)	B1—O3	1.381 (4)
Tb1—O2^{ii}	2.336 (4)	B1—O3^{vii}	1.381 (6)
Tb1—O2^{iii}	2.336 (6)	B1—O3^{viii}	1.381 (6)
Tb1—O2^{iv}	2.336 (4)	O1—B2	1.389 (8)
Tb1—O2^{v}	2.336 (4)	O2—B2^{ix}	1.362 (12)
Tb1—O2^{vi}	2.336 (6)		
O2^{i}—Tb1—O2^{ii}	89.15 (16)	O2^{iii}—Tb1—O2^{vi}	144.93 (12)
O2^{i}—Tb1—O2^{iii}	89.15 (16)	O2^{iv}—Tb1—O2^{v}	89.15 (16)
O2^{i}—Tb1—O2^{iv}	119.88 (12)	O2^{iv}—Tb1—O2^{vi}	89.15 (16)
O2^{i}—Tb1—O2^{v}	144.93 (19)	O2^{v}—Tb1—O2^{vi}	89.15 (16)
O2^{i}—Tb1—O2^{vi}	73.32 (15)	O3—B1—O3^{vii}	120.0 (4)
O2^{ii}—Tb1—O2^{iii}	89.15 (16)	O3—B1—O3^{viii}	120.0 (4)
O2^{ii}—Tb1—O2^{iv}	144.93 (19)	O3^{vii}—B1—O3^{viii}	120.0 (4)
O2^{ii}—Tb1—O2^{v}	73.32 (14)	Tb1^{x}—O2—B2^{ix}	105.0 (3)
O2^{ii}—Tb1—O2^{vi}	119.88 (18)	O1—B2—O2^{xi}	117.7 (9)
O2^{iii}—Tb1—O2^{iv}	73.32 (15)	O1—B2—O2^{xii}	117.7 (9)
O2^{iii}—Tb1—O2^{v}	119.88 (18)	O2^{xi}—B2—O2^{xii}	124.7 (6)

Symmetry codes: (i) *x*−1/3, *y*+1/3, *z*+1/3; (ii) −*y*−1/3, *x*−*y*−2/3, *z*+1/3; (iii) −*x*+*y*+2/3, −*x*+1/3, *z*+1/3; (iv) *y*+1/3, *x*−1/3, −*z*−1/3; (v) *x*−*y*−2/3, −*y*−1/3, −*z*−1/3; (vi) −*x*+1/3, −*x*+*y*+2/3, −*z*−1/3; (vii) −*y*+1, *x*−*y*, *z*; (viii) −*x*+*y*+1, −*x*+1, *z*; (ix) *x*−2/3, *y*−1/3, *z*−1/3; (x) *x*+1/3, *y*−1/3, *z*−1/3; (xi) *x*+2/3, *y*+1/3, *z*+1/3; (xii) *y*+1, *x*, −*z*.

Dysprosium trialuminium tetrakis(borate) (Dy-borate)

Crystal data

$DyAl_3(BO_3)_4$
$M_r = 478.7$
Trigonal, *R*32
Hall symbol: R 3 2"
$a = 9.2938$ (5) Å
$c = 7.2348$ (4) Å
$V = 541.18$ (5) Å^3
$Z = 3$
$F(000) = 663$
$D_x = 4.406$ Mg m^{-3}
Mo $K\alpha$ radiation, $\lambda = 0.71075$ Å
Cell parameters from 7295 reflections
$\theta = 3.8$–$31.5°$
$\mu = 10.81$ mm^{-1}
$T = 100$ K
Hexagonal prism, light white
0.05 × 0.05 × 0.03 mm

Data collection

Bruker D8 QUEST CMOS area detector diffractometer
Radiation source: X-ray tube
φ and ω scans
Absorption correction: multi-scan (SADABS; Krause *et al.*, 2015)
$T_{min} = 0.588$, $T_{max} = 0.723$
7295 measured reflections
420 independent reflections
420 reflections with $I > 2\sigma(I)$
$R_{int} = 0.044$
$\theta_{max} = 31.5°$, $\theta_{min} = 3.8°$
$h = -12 \rightarrow 13$
$k = -13 \rightarrow 13$
$l = -10 \rightarrow 10$

Refinement

Refinement on *F*
$R[F > 3\sigma(F)] = 0.010$
$wR(F) = 0.010$
$S = 1.14$
420 reflections
35 parameters
0 restraints
0 constraints
Primary atom site location: iterative
Weighting scheme based on measured s.u.'s $w = 1/(\sigma^2(F) + 0.0001F^2)$
$(\Delta/\sigma)_{max} = 0.017$
$\Delta\rho_{max} = 0.29$ e Å^{-3}
$\Delta\rho_{min} = -0.39$ e Å^{-3}
Absolute structure: The crystal had chiral structure. Data was refined with inversion twinning in JANA2006, and the twin ratio was 0.509(8):0.491(8).
Absolute structure parameter: 0.491 (8)

Special details

Refinement. Data was refined with inversion twinning, and the twin ratio was 0.509 (8):0.491 (8).

Fractional atomic coordinates and isotropic or equivalent isotropic displacement parameters (Å^2)

	x	*y*	*z*	U_{iso}*/U_{eq}
Dy1	0	0	0	0.00585 (4)
Al1	0.55590 (10)	0	0	0.0031 (2)
O1	0.7422 (3)	0.0755 (3)	0.166667	0.0084 (9)
B1	0.666667	0.333333	−0.166667	0.0062 (7)
O3	0.36691 (18)	−0.11579 (17)	−0.14502 (18)	0.0065 (4)
O2	0.8159 (2)	0.4825 (2)	−0.166667	0.0067 (5)
B2	0.8916 (5)	0.2249 (5)	0.166667	0.0063 (10)

Atomic displacement parameters (Å^2)

	U^{11}	U^{22}	U^{33}	U^{12}	U^{13}	U^{23}
Dy1	0.00546 (6)	0.00546 (6)	0.00665 (6)	0.00273 (3)	0	0

Al1	0.0027 (2)	0.0023 (3)	0.0042 (3)	0.00114 (15)	−0.00007 (10)	−0.0001 (2)
O1	0.0075 (11)	0.0075 (11)	0.0082 (10)	0.0022 (11)	−0.0006 (4)	0.0006 (4)
B1	0.0068 (9)	0.0068 (9)	0.0051 (13)	0.0034 (4)	0	0
O3	0.0058 (6)	0.0063 (5)	0.0072 (5)	0.0029 (4)	−0.0011 (4)	−0.0013 (4)
O2	0.0060 (6)	0.0060 (6)	0.0071 (7)	0.0022 (7)	−0.0004 (3)	0.0004 (3)
B2	0.0083 (11)	0.0083 (11)	0.0058 (9)	0.0068 (15)	−0.0001 (5)	0.0001 (5)

Geometric parameters (Å, º)

Dy1—O3^{i}	2.3260 (16)	Al1—Al1^{viii}	2.9992 (7)
Dy1—O3^{ii}	2.3260 (13)	O1—B2	1.388 (4)
Dy1—O3^{iii}	2.326 (2)	B1—O2	1.3866 (13)
Dy1—O3^{iv}	2.3260 (16)	B1—O2^{ix}	1.387 (2)
Dy1—O3^{v}	2.3260 (13)	B1—O2^{x}	1.387 (2)
Dy1—O3^{vi}	2.326 (2)	O3—B2^{xi}	1.364 (6)
Al1—Al1^{vii}	2.9992 (7)		
O3^{i}—Dy1—O3^{ii}	89.16 (6)	O3^{iv}—Dy1—O3^{v}	89.16 (6)
O3^{i}—Dy1—O3^{iii}	89.16 (6)	O3^{iv}—Dy1—O3^{vi}	89.16 (6)
O3^{i}—Dy1—O3^{iv}	119.78 (5)	O3^{v}—Dy1—O3^{vi}	89.16 (6)
O3^{i}—Dy1—O3^{v}	145.03 (7)	Al1^{vii}—Al1—Al1^{viii}	118.02 (3)
O3^{i}—Dy1—O3^{vi}	73.33 (6)	O2—B1—O2^{ix}	120.00 (13)
O3^{ii}—Dy1—O3^{iii}	89.16 (6)	O2—B1—O2^{x}	120.00 (13)
O3^{ii}—Dy1—O3^{iv}	145.03 (7)	O2^{ix}—B1—O2^{x}	120.00 (13)
O3^{ii}—Dy1—O3^{v}	73.33 (5)	Dy1^{xii}—O3—B2^{xi}	105.29 (15)
O3^{ii}—Dy1—O3^{vi}	119.78 (7)	O1—B2—O3^{xiii}	117.3 (4)
O3^{iii}—Dy1—O3^{iv}	73.33 (6)	O1—B2—O3^{xiv}	117.3 (4)
O3^{iii}—Dy1—O3^{v}	119.78 (7)	O3^{xiii}—B2—O3^{xiv}	125.4 (3)
O3^{iii}—Dy1—O3^{vi}	145.03 (5)		

Symmetry codes: (i) $x-1/3, y+1/3, z+1/3$; (ii) $-y-1/3, x-y-2/3, z+1/3$; (iii) $-x+y+2/3, -x+1/3, z+1/3$; (iv) $y+1/3, x-1/3, -z-1/3$; (v) $x-y-2/3, -y-1/3, -z-1/3$; (vi) $-x+1/3, -x+y+2/3, -z-1/3$; (vii) $-y+2/3, x-y-2/3, z+1/3$; (viii) $-x+y+4/3, -x+2/3, z-1/3$; (ix) $-y+1, x-y, z$; (x) $-x+y+1, -x+1, z$; (xi) $x-2/3, y-1/3, z-1/3$; (xii) $x+1/3, y-1/3, z-1/3$; (xiii) $x+2/3, y+1/3, z+1/3$; (xiv) $y+1, x, -z$.

Holmium trialuminium tetrakis(borate) (Ho-borate)

Crystal data

$HoAl_3(BO_3)_4$
M_r = 481.1
Trigonal, *R*32
Hall symbol: R 3 2"
a = 9.2832 (3) Å
c = 7.2345 (3) Å
V = 539.93 (3) Å^3
Z = 3
F(000) = 666

D_x = 4.439 Mg m^{-3}
Mo *Kα* radiation, λ = 0.71075 Å
Cell parameters from 5662 reflections
θ = 3.8–30.5°
μ = 11.45 mm^{-1}
T = 100 K
Hexagonal prism, light pink
0.05 × 0.05 × 0.03 mm

Data collection

Bruker D8 QUEST CMOS area detector diffractometer
Radiation source: X-ray tube
φ and ω scans

Absorption correction: multi-scan (SADABS; Krause *et al.*, 2015)
T_{min} = 0.570, T_{max} = 0.709
5662 measured reflections

381 independent reflections
381 reflections with $I > 2\sigma(I)$
$R_{int} = 0.047$
$\theta_{max} = 30.5°$, $\theta_{min} = 3.8°$
$h = -13 \rightarrow 13$
$k = -13 \rightarrow 12$
$l = -10 \rightarrow 10$

Refinement

Refinement on F
$R[F > 3\sigma(F)] = 0.012$
$wR(F) = 0.015$
$S = 1.08$
381 reflections
35 parameters
0 restraints
0 constraints
Primary atom site location: iterative
Weighting scheme based on measured s.u.'s $w = 1/(\sigma^2(F) + 0.0001F^2)$
$(\Delta/\sigma)_{max} = 0.036$
$\Delta\rho_{max} = 0.54$ e Å^{-3}
$\Delta\rho_{min} = -0.65$ e Å^{-3}
Absolute structure: The crystal had chiral structure. Data was refined with inversion twinning in JANA2006, and the twin ratio was 0.558(12):0.442(12).
Absolute structure parameter: 0.442 (12)

Special details

Refinement. Data was refined with inversion twinning, and the twin ratio was 0.558 (12):0.442 (12).

Fractional atomic coordinates and isotropic or equivalent isotropic displacement parameters (Å²)

	x	*y*	*z*	U_{iso}*/U_{eq}
Ho1	0	0	0	0.01041 (7)
Al1	0.55519 (15)	0	0	0.0062 (3)
B1	0.666667	0.333333	−0.166667	0.0090 (12)
O1	0.7428 (5)	0.0762 (5)	0.166667	0.0123 (14)
O3	0.3668 (3)	−0.1161 (3)	−0.1461 (3)	0.0101 (7)
O2	0.8155 (3)	0.4822 (3)	−0.166667	0.0094 (8)
B2	0.8911 (8)	0.2245 (8)	0.166667	0.0105 (16)

Atomic displacement parameters (Å²)

	U^{11}	U^{22}	U^{33}	U^{12}	U^{13}	U^{23}
Ho1	0.00996 (9)	0.00996 (9)	0.01130 (10)	0.00498 (4)	0	0
Al1	0.0058 (4)	0.0056 (5)	0.0071 (5)	0.0028 (2)	−0.00023 (15)	−0.0005 (3)
B1	0.0105 (15)	0.0105 (15)	0.0060 (18)	0.0053 (8)	0	0
O1	0.0107 (17)	0.0107 (17)	0.0140 (16)	0.0044 (17)	−0.0021 (7)	0.0021 (7)
O3	0.0100 (10)	0.0098 (9)	0.0106 (7)	0.0050 (7)	−0.0004 (6)	−0.0009 (7)
O2	0.0078 (9)	0.0078 (9)	0.0119 (10)	0.0033 (11)	0.0000 (5)	0.0000 (5)
B2	0.0131 (18)	0.0131 (18)	0.0090 (15)	0.009 (2)	0.0006 (9)	−0.0006 (9)

Geometric parameters (Å, º)

Ho1—O3^{i}	2.318 (3)	B1—O2	1.382 (2)
Ho1—O3^{ii}	2.318 (2)	B1—O2^{vii}	1.382 (4)
Ho1—O3^{iii}	2.318 (3)	B1—O2^{viii}	1.382 (4)
Ho1—O3^{iv}	2.318 (3)	O1—B2	1.377 (6)
Ho1—O3^{v}	2.318 (2)	O3—B2^{ix}	1.364 (9)
Ho1—O3^{vi}	2.318 (3)		

O3^{i}—Ho1—O3^{ii}	89.28 (9)	O3^{iii}—Ho1—O3^{vi}	144.97 (7)
O3^{i}—Ho1—O3^{iii}	89.28 (9)	O3^{iv}—Ho1—O3^{v}	89.28 (9)
O3^{i}—Ho1—O3^{iv}	119.73 (7)	O3^{iv}—Ho1—O3^{vi}	89.28 (9)
O3^{i}—Ho1—O3^{v}	144.97 (12)	O3^{v}—Ho1—O3^{vi}	89.28 (9)
O3^{i}—Ho1—O3^{vi}	73.16 (9)	O2—B1—O2^{vii}	120.0 (2)
O3^{ii}—Ho1—O3^{iii}	89.28 (9)	O2—B1—O2^{viii}	120.0 (2)
O3^{ii}—Ho1—O3^{iv}	144.97 (12)	O2^{vii}—B1—O2^{viii}	120.0 (2)
O3^{ii}—Ho1—O3^{v}	73.16 (8)	Ho1^{x}—O3—B2^{ix}	105.5 (2)
O3^{ii}—Ho1—O3^{vi}	119.73 (11)	O1—B2—O3^{xi}	117.4 (7)
O3^{iii}—Ho1—O3^{iv}	73.16 (9)	O1—B2—O3^{xii}	117.4 (7)
O3^{iii}—Ho1—O3^{v}	119.73 (11)	O3^{xi}—B2—O3^{xii}	125.3 (4)

Symmetry codes: (i) $x-1/3, y+1/3, z+1/3$; (ii) $-y-1/3, x-y-2/3, z+1/3$; (iii) $-x+y+2/3, -x+1/3, z+1/3$; (iv) $y+1/3, x-1/3, -z-1/3$; (v) $x-y-2/3, -y-1/3, -z-1/3$; (vi) $-x+1/3, -x+y+2/3, -z-1/3$; (vii) $-y+1, x-y, z$; (viii) $-x+y+1, -x+1, z$; (ix) $x-2/3, y-1/3, z-1/3$; (x) $x+1/3, y-1/3, z-1/3$; (xi) $x+2/3, y+1/3, z+1/3$; (xii) $y+1, x, -z$.